

An extremely low mass ratio contact binary NW Aps with a potential compact companion star

Xiao Zhou,^{1,2,3}★

¹Yunnan Observatories, Chinese Academy of Sciences (CAS), P.O. Box 110, 650216 Kunming, China

²Key Laboratory of the Structure and Evolution of Celestial Objects, Chinese Academy of Sciences, P. O. Box 110, 650216 Kunming, China

³Center for Astronomical Mega-Science, Chinese Academy of Sciences, 20A Datun Road, Chaoyang District, Beijing, 100012, China

Accepted XXX. Received YYY; in original form ZZZ

ABSTRACT

The photometric solutions of NW Aps reveal that it is a low mass ratio ($q = 0.086$) contact binary system. Investigation of orbital period shows that its orbital period is increasing continuously at a rate of $dP/dt = +1.117(\pm 0.005) \times 10^{-6} \text{ day} \cdot \text{year}^{-1}$, which may be caused by mass transfer from the less massive component to the more massive one at a rate of $\frac{dM_2}{dt} = -3.36(\pm 0.02) \times 10^{-8} M_{\odot}/\text{year}$. A cyclic variation of $P_3 = 22.9(\pm 0.1)$ is also found in the O - C curve. There may be a potential compact object orbiting around NW Aps, with its minimum mass to be $M_3 = 0.436(\pm 0.007) M_{\odot}$. However, the magnetic activity of the primary star may also account for the cyclic change. NW Aps is a stellar merger candidate with the longest orbital period among all stellar merge candidates with mass ratio $q < 0.1$. It is still in a stable state since the ratio of orbital angular momentum (J_{orb}) to spin angular momentum (J_{spin}) is $\frac{J_{orb}}{J_{spin}} = 3.257$. Both of its primary and secondary star are oversized to main sequence stars, and the surface gravity of the primary and secondary stars are significant lower than main sequence stars. The P - log g relationship is fitted with parabola for low mass ratio contact binary systems. More targets laid in the gap are needed to confirm the P - log g relationship and reveal the final evolutionary state of low mass ratio contact binary system.

Key words: binaries: eclipsing – stars: fundamental parameters – stars: evolution – stars: individuals (NW Aps)

1 INTRODUCTION

Stellar mergers are predicted to be common events in the Galaxy (Kochanek et al. 2014). However, only a handful number of these transients have been noted so far, which are the merger events of V4332 Sgr (Hayashi et al. 1994), V838 Mon (Brown et al. 2002), V1309 Sco (Nakano et al. 2008), and OGLE-2002-BLG-360 (Tylenda et al. 2013). Common envelope evolution and stellar merger is a very important formation channel for peculiar stars, following with luminous transients (Ivanova et al. 2013; Pejcha et al. 2016). For example, the formation of blue stragglers have been debated for a long time (Chen & Han 2008), and one possible explanation is that they are products of binary merger. The merger event of V1309 Sco was observed on 2008. Its light curves in I band were observed by OGLE on 2004, which revealed that it was a contact binary with extremely low mass ratio ($q = 0.094$) before merger (Zhu et al. 2016). V1309 Sco was observed with infrared CCD recently, which showed that reasonable equilibrium in this stellar merger remnant was being reached in about 9 years after the outburst. V1309 Sco has settled into a nearly constant magnitude, resembling a normal blue star. The asymptotic blue color of V1309 Sco as the resultant of a stellar merger event suggests that the object is a blue straggler in the making, as theoretically predicted (Ferreira et al. 2019).

The discovery of the luminous red nova V1309 Sco (Nova Scorpii 2008) and the fact that its progenitor was an extreme mass ratio contact binary system inspired researchers to search stellar merger candidates in low mass ratio overcontact binary system (Qian et al. 2011; Gazeas et al. 2021; Christopoulou et al. 2022). Owe to the large sky survey projects such as the Optical Gravitational Lensing Experiment (OGLE) (Udalski et al. 1992), All Sky Automated Survey (ASAS) (Pojmanski 1997), Wide-field Infrared Survey Explorer (WISE) (Chen et al. 2018), Transiting Exoplanet Survey Satellite (TESS) (Ricker et al. 2015; Prša et al. 2022) and Zwicky Transient Facility (ZTF) (Bellm et al. 2019; Chen et al. 2020), the light curves of contact binaries are accumulating rapidly. However, only a few tens of low mass ratio contact binaries have been identified (Yang & Qian 2015; Christopoulou et al. 2022). Hut (1980) revealed that low mass ratio contact binary system with a decreasing period will evolve into a rapidly rotating single star when the photosphere surface of the binary system was close to the outer critical Roche lobe, while system with an increasing period may merge when it met the criterion that the orbital angular momentum was less than 3 times of the total spin angular momentum. Theoretical models predicted that a contact binary system will unstable and merge when its mass ratio reached around $q \sim 0.07 - 0.09$ (Arbutina 2007).

In the present work, we will report our research of a low mass ratio contact binary system NW Aps ($V = 9^m.08 - 9^m.37$, $P = 1.065558$ days), which has the longest orbital period in all low mass ratio contact binary systems to date. Its light variability was first noted by

★ E-mail: zhouxiaophy@ynao.ac.cn

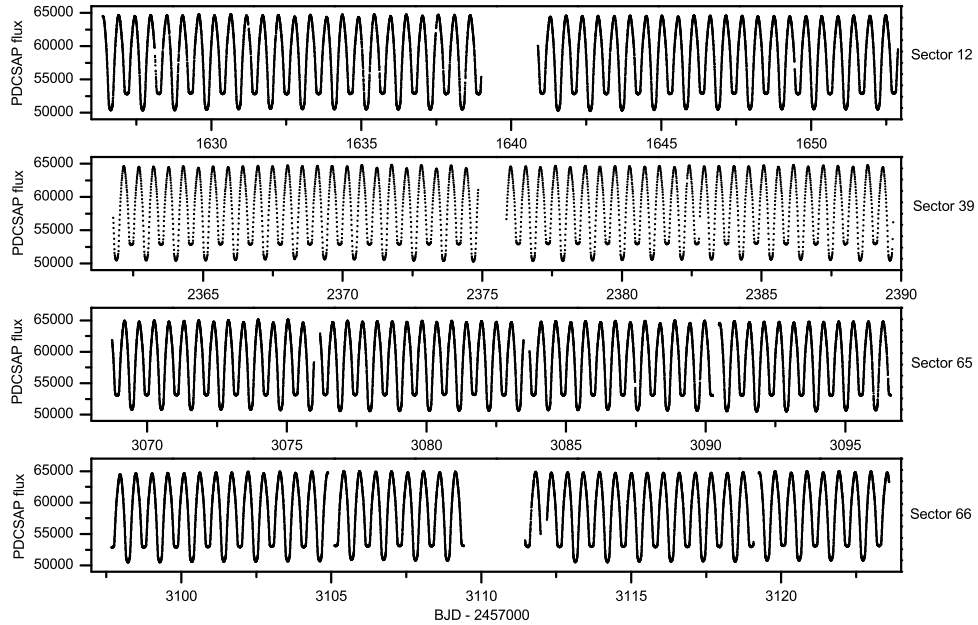


Figure 1. Light curves of TIC 359987981 from Sector 12, 39, 65 and 66.

[Strohmeier & Patterson \(1969\)](#), named as HD 130338. The target was neglected until its V band light curve from ASAS was analysed by [Wadhwa \(2005\)](#). [Wadhwa \(2005\)](#) reported that the mass ratio of NW Aps was $q = 0.100(\pm 0.002)$, making it a stellar merger candidate. No more detailed study was carried out after that. Fortunately, it is a quite bright star listed in TESS two-minute target lists as TIC 359987981. Thus, we can acquire its full light curves with very high precision. Its light curves from TESS are displayed in Section 2, and orbital period variations are investigated in Section 3. The light curves are modelled in Section 4. The Spectral Energy Distribution of NW Aps is synthesized in Section 5. Discussions and Conclusions are arranged in Section 6 and Section 7, respectively.

2 TESS OBSERVATIONS

TESS is a sky survey telescope optimized for detecting exoplanets, which was launched on April, 2018. It is equipped with four cameras which covers a quite large field of view (24×96 degree), and use a wide bandpass filter with its wavelength ranging from nearly 600 to 1000 nm. TESS has been monitoring the whole sky for over six years. The observations for each sector lasting for about 27.4 days, which makes it to be a very suitable telescope for searching close binaries.

TIC 359987981 was observed by TESS with 2 minutes cadence in Sector 12 extending from 2019 May 21 to 2019 June 18, Sector 65 extending from 2023 May 4 to 2023 June 1, Sector 66 extending from 2023 June 2 to 2023 July 1, and with 10 minutes cadence in Sector 39 extending from May 27 through June 24, 2021. The light curves are downloaded from the MAST data archive (<https://archive.stsci.edu/>) using the Python package `lightkurve` ([Lightkurve Collaboration et al. 2018](#)). The light curves extracted with TESS data processing pipeline developed by the Science Processing Operations Center (SPOC) with an exposure time of 120 seconds are downloaded for Sector 12, Sector 65 and Sector 66 ([Jenkins et al. 2016](#)). The light curves extracted with TESS Light Curves From Full Frame Images (TESS-SPOC) pipeline ([Caldwell et al. 2020](#)) with an exposure time of 600 seconds are downloaded for Sector 39. Both the Simple Aperture Photometry (SAP) flux and Pre-search Data Conditioning SAP flux (PDCSAP) flux are provided in TESS light curves. The SAP flux is calculated by summing the brightness of all chosen pixels, while long term trends have been removed in the PDCSAP flux. Thus, PDCSAP flux is usually cleaner than the SAP flux and will have fewer systematic trends. The Pre-search Data Conditioning Simple Aperture Photometry (PDCSAP) flux are used in the present work. The observational light curves of TIC 359987981 are displayed in Fig. 1.

3 INVESTIGATION OF ORBITAL PERIOD VARIATIONS

Contact binaries are typical interaction binary systems. Due to the possible mass transfer between their component stars, long term period changes commonly appear in contact binary systems. [Huang \(1963\)](#) discussed mass ejection in binary systems and predicted their effect on the orbital period of the systems. [Qian \(2001\)](#) reported that a relation between the period change and the mass ratio may exist, basing on the research of the period changes of 30 W-type contact binaries. The period of NW Aps was given to be $P = 1.065558$ days by [Wadhwa](#)

(2005). Times of minima determined by other researchers are collected, which are HJD 2448500.6490 (Paschke 2009), HJD 2451967.9590 (O - C gateway, <http://var2.astro.cz/ocgate/>), HJD 2452728.7720 (GCVS, <http://www.sai.msu.su/gcvs/gcvs/>), HJD 2454984.5480 and HJD 2455390.5250 (Paschke 2010). A total of 186 times of minima are determined from the light curves displayed in Fig. 1, which are all listed in Table 1. And the times of light minima are computed using the method introduced by Kwee & van Woerden (1956). The Kwee & van Woerden (K - W) method is a classical and widely used technique for determining the times of light minima in eclipsing binary light curves. Before the computing, we should choose a phase interval from a single eclipse's observational data, which covers both the descending and ascending branches. Then, we interpolate the observational data to $2n + 1$ equally spaced points with a time interval of Δt , and an initial epoch of minimum T_1 is selected. The number of interpolated in-eclipse observations $2n + 1$ is recommended to be about equal to the total number of observations in the phase interval. Take T_1 as reflection axis and reflect the interpolated magnitudes of the descending branch to the ascending branch, and calculate the magnitude differences Δm_k ($k = 1, \dots, n$) to get $s(T_1) = \sum_{k=1}^n (\Delta m_k)^2$. Assuming $s(T) = aT^2 + bT + c$, and shift the reflection axis to $T_1 + \frac{1}{2}\Delta t$ and $T_1 - \frac{1}{2}\Delta t$ to compute $s(T_1 + \frac{1}{2}\Delta t)$ and $s(T_1 - \frac{1}{2}\Delta t)$. Using the three s -values corresponding to $T_1 - \frac{1}{2}\Delta t$, T_1 and $T_1 + \frac{1}{2}\Delta t$, the coefficients a, b, c will be determined. The Epoch of light minimum is calculated as $T_0 = -\frac{b}{2a}$ and its mean error is given by $\sigma_{T_0}^2 = \frac{4ac - b^2}{4a^2(Z-1)}$, where Z is the number of independent magnitude pairs. The times of minima determined from the TESS data and those collected from literature are used to investigate the period variations of NW Aps. The minima in HJD are converted to BJD since TESS used BJD time system and all times of minima are listed in Table 1. All times of minima are determined from observations obtained with charge-coupled device (CCD) photometry. The time of primary light minimum BJD 2458626.6484 is adopted as the initial time since it is determined with TESS observations, which has very high accuracy. Thus, the linear equation used to calculate the $O - C$ values is:

$$Min.I(BJD) = 2458626.6484 + 1^d.065558 \times E. \quad (1)$$

The column to column description of Table 1 are:

- Column 1 - Barycentric Julian Date of the observed times of minima (BJD - 2400000);
- Column 2 - primary (p) or secondary (s) minima;
- Column 3 - error of times of minima;
- Column 4 - cycle numbers from the initial epoch (E, as used in Equation 1);
- Column 5 - the $O - C$ values calculated from linear Equation 1;
- Column 6 - the references;

Table 1: Times of minima and $O - C$ values for NW Aps.

BJD (2400000+)	p/s	Error (days)	Epoch (days)	$O - C$ (days)	Ref.	BJD (2400000+)	p/s	Error (days)	Epoch (days)	$O - C$ (days)	Ref.
48500.6497	p		-9503	-0.0011	1	59387.4741	p	0.0007	714	0.0172	5
51967.9598	p		-6249	-0.0167	2	59388.0083	s	0.0007	714.5	0.0187	5
52728.7728	p		-5535	-0.0122	3	59388.5396	p	0.0006	715	0.0172	5
54984.5488	p	0.0100	-3418	-0.0225	4	59389.0737	s	0.0007	715.5	0.0185	5
55390.5258	p	0.0100	-3037	-0.0230	4	60068.9193	s	0.0003	1353.5	0.0381	5
58626.6484	p	0.0003	0	0	5	60069.4515	p	0.0003	1354	0.0375	5
58627.1828	s	0.0003	0.5	0.0016	5	60069.9848	s	0.0003	1354.5	0.0380	5
58627.7144	p	0.0003	1	0.0004	5	60070.5168	p	0.0003	1355	0.0373	5
58628.2480	s	0.0004	1.5	0.0012	5	60071.0503	s	0.0003	1355.5	0.0380	5
58628.7809	p	0.0003	2	0.0013	5	60071.5820	p	0.0003	1356	0.0369	5
58629.3132	s	0.0003	2.5	0.0009	5	60072.1166	s	0.0003	1356.5	0.0387	5
58629.8461	p	0.0003	3	0.0010	5	60072.6473	p	0.0003	1357	0.0367	5
58630.3790	s	0.0003	3.5	0.0011	5	60073.1823	s	0.0003	1357.5	0.0389	5
58630.9119	p	0.0003	4	0.0012	5	60073.7122	p	0.0003	1358	0.0360	5
58631.4448	s	0.0003	4.5	0.0014	5	60074.2483	s	0.0003	1358.5	0.0393	5
58631.9765	p	0.0003	5	0.0003	5	60074.7779	p	0.0003	1359	0.0362	5
58632.5108	s	0.0003	5.5	0.0018	5	60075.3140	s	0.0003	1359.5	0.0395	5
58633.0416	p	0.0003	6	-0.0002	5	60075.8438	p	0.0003	1360	0.0364	5
58633.5767	s	0.0003	6.5	0.0021	5	60076.3792	s	0.0003	1360.5	0.0391	5
58634.1068	p	0.0003	7	-0.0005	5	60076.9097	p	0.0003	1361	0.0369	5
58634.6427	s	0.0003	7.5	0.0026	5	60077.4447	s	0.0003	1361.5	0.0390	5
58635.1721	p	0.0003	8	-0.0008	5	60077.9759	p	0.0003	1362	0.0374	5
58635.7083	s	0.0003	8.5	0.0026	5	60078.5101	s	0.0003	1362.5	0.0389	5
58636.2384	p	0.0003	9	-0.0001	5	60079.0416	p	0.0003	1363	0.0376	5
58636.7735	s	0.0003	9.5	0.0022	5	60079.5751	s	0.0003	1363.5	0.0384	5
58637.3044	p	0.0003	10	0.0003	5	60080.1079	p	0.0003	1364	0.0383	5
58637.8388	s	0.0003	10.5	0.0020	5	60080.6405	s	0.0003	1364.5	0.0382	5
58638.3702	p	0.0003	11	0.0007	5	60081.1732	p	0.0003	1365	0.0381	5
58641.0356	s	0.0003	13.5	0.0021	5	60081.7061	s	0.0003	1365.5	0.0382	5

Table 1 continued

BJD (2400000+)	p/s	Error (days)	Epoch (days)	$O - C$ (days)	Ref.	BJD (2400000+)	p/s	Error (days)	Epoch (days)	$O - C$ (days)	Ref.
58641.5664	p	0.0003	14	0.0001	5	60082.2387	p	0.0003	1366	0.0380	5
58642.1008	s	0.0003	14.5	0.0018	5	60082.7725	s	0.0003	1366.5	0.0391	5
58642.6323	p	0.0003	15	0.0005	5	60083.3035	p	0.0003	1367	0.0373	5
58643.1657	s	0.0003	15.5	0.0011	5	60083.8382	s	0.0003	1367.5	0.0392	5
58643.6980	p	0.0003	16	0.0006	5	60084.3689	p	0.0003	1368	0.0371	5
58644.2321	s	0.0003	16.5	0.0020	5	60084.9038	s	0.0003	1368.5	0.0393	5
58644.7640	p	0.0003	17	0.0011	5	60085.4342	p	0.0003	1369	0.0369	5
58645.2984	s	0.0003	17.5	0.0027	5	60085.9694	s	0.0003	1369.5	0.0393	5
58645.8292	p	0.0003	18	0.0007	5	60086.4998	p	0.0003	1370	0.0369	5
58646.3635	s	0.0003	18.5	0.0022	5	60087.0350	s	0.0003	1370.5	0.0394	5
58646.8948	p	0.0003	19	0.0007	5	60087.5654	p	0.0003	1371	0.0370	5
58647.4287	s	0.0003	19.5	0.0019	5	60088.1008	s	0.0003	1371.5	0.0396	5
58647.9605	p	0.0003	20	0.0009	5	60088.6310	p	0.0003	1372	0.0370	5
58648.4939	s	0.0003	20.5	0.0016	5	60089.1666	s	0.0003	1372.5	0.0398	5
58649.0256	p	0.0003	21	0.0005	5	60089.6967	p	0.0003	1373	0.0371	5
58649.5591	s	0.0003	21.5	0.0011	5	60090.7625	p	0.0003	1374	0.0374	5
58650.0916	p	0.0003	22	0.0009	5	60091.2972	s	0.0003	1374.5	0.0393	5
58650.6257	s	0.0003	22.5	0.0022	5	60091.8284	p	0.0003	1375	0.0377	5
58651.1567	p	0.0003	23	0.0004	5	60092.3625	s	0.0003	1375.5	0.0390	5
58651.6911	s	0.0003	23.5	0.0021	5	60092.8944	p	0.0003	1376	0.0382	5
58652.2227	p	0.0003	24	0.0008	5	60093.4278	s	0.0003	1376.5	0.0387	5
58652.7568	s	0.0003	24.5	0.0022	5	60093.9601	p	0.0003	1377	0.0383	5
59362.4342	s	0.0007	690.5	0.0180	5	60094.4935	s	0.0003	1377.5	0.0389	5
59362.9658	p	0.0006	691	0.0168	5	60095.0256	p	0.0003	1378	0.0382	5
59363.4999	s	0.0007	691.5	0.0181	5	60095.5597	s	0.0003	1378.5	0.0396	5
59364.0312	p	0.0006	692	0.0166	5	60096.0907	p	0.0003	1379	0.0377	5
59364.5661	s	0.0007	692.5	0.0188	5	60098.2220	p	0.0003	1381	0.0379	5
59365.0969	p	0.0007	693	0.0168	5	60098.7557	s	0.0003	1381.5	0.0389	5
59365.6307	s	0.0007	693.5	0.0178	5	60099.2875	p	0.0003	1382	0.0379	5
59366.1629	p	0.0007	694	0.0172	5	60099.8218	s	0.0003	1382.5	0.0394	5
59366.6964	s	0.0007	694.5	0.0180	5	60100.3533	p	0.0003	1383	0.0382	5
59367.2282	p	0.0007	695	0.0169	5	60100.8872	s	0.0003	1383.5	0.0392	5
59367.7615	s	0.0007	695.5	0.0175	5	60101.4191	p	0.0003	1384	0.0384	5
59368.2942	p	0.0007	696	0.0174	5	60101.9527	s	0.0003	1384.5	0.0392	5
59368.8275	s	0.0007	696.5	0.0179	5	60102.4854	p	0.0003	1385	0.0391	5
59369.3589	p	0.0007	697	0.0165	5	60103.0179	s	0.0003	1385.5	0.0389	5
59369.8932	s	0.0007	697.5	0.0180	5	60103.5507	p	0.0003	1386	0.0389	5
59370.4237	p	0.0007	698	0.0158	5	60104.0837	s	0.0003	1386.5	0.0391	5
59370.9601	s	0.0007	698.5	0.0194	5	60104.6165	p	0.0003	1387	0.0391	5
59371.4892	p	0.0007	699	0.0157	5	60105.6816	p	0.0003	1388	0.0386	5
59372.0253	s	0.0007	699.5	0.0190	5	60106.2153	s	0.0003	1388.5	0.0396	5
59372.5548	p	0.0007	700	0.0158	5	60106.7469	p	0.0003	1389	0.0384	5
59373.0913	s	0.0007	700.5	0.0195	5	60107.2813	s	0.0003	1389.5	0.0400	5
59373.6207	p	0.0007	701	0.0161	5	60107.8119	p	0.0003	1390	0.0378	5
59374.1558	s	0.0007	701.5	0.0184	5	60108.3463	s	0.0003	1390.5	0.0394	5
59374.6866	p	0.0007	702	0.0165	5	60108.8779	p	0.0003	1391	0.0383	5
59376.2871	s	0.0007	703.5	0.0186	5	60112.6089	s	0.0003	1394.5	0.0398	5
59376.8187	p	0.0007	704	0.0174	5	60113.1408	p	0.0003	1395	0.0389	5
59377.3523	s	0.0007	704.5	0.0182	5	60113.6743	s	0.0003	1395.5	0.0397	5
59377.8848	p	0.0007	705	0.0180	5	60114.2067	p	0.0003	1396	0.0393	5
59378.4176	s	0.0007	705.5	0.0180	5	60114.7402	s	0.0003	1396.5	0.0400	5
59378.9498	p	0.0007	706	0.0175	5	60115.2715	p	0.0003	1397	0.0385	5
59379.4835	s	0.0007	706.5	0.0183	5	60115.8055	s	0.0003	1397.5	0.0397	5
59380.0152	p	0.0007	707	0.0173	5	60116.3371	p	0.0003	1398	0.0386	5
59380.5492	s	0.0007	707.5	0.0184	5	60116.8713	s	0.0003	1398.5	0.0400	5
59381.0805	p	0.0007	708	0.0170	5	60117.4024	p	0.0003	1399	0.0384	5
59381.6147	s	0.0007	708.5	0.0184	5	60117.9364	s	0.0003	1399.5	0.0395	5
59382.1461	p	0.0007	709	0.0170	5	60118.4677	p	0.0003	1400	0.0380	5

Table 1 continued

BJD (2400000+)	p/s	Error (days)	Epoch (days)	$O - C$ (days)	Ref.	BJD (2400000+)	p/s	Error (days)	Epoch (days)	$O - C$ (days)	Ref.
59382.6802	s	0.0008	709.5	0.0184	5	60119.5338	p	0.0003	1401	0.0386	5
59383.2120	p	0.0007	710	0.0173	5	60120.0683	s	0.0003	1401.5	0.0403	5
59383.7465	s	0.0007	710.5	0.0191	5	60120.5992	p	0.0003	1402	0.0384	5
59384.2778	p	0.0007	711	0.0176	5	60121.1337	s	0.0003	1402.5	0.0402	5
59384.8103	s	0.0007	711.5	0.0174	5	60121.6648	p	0.0003	1403	0.0385	5
59385.3435	p	0.0007	712	0.0178	5	60122.1997	s	0.0003	1403.5	0.0406	5
59385.8765	s	0.0007	712.5	0.0180	5	60122.7308	p	0.0003	1404	0.0389	5
59386.4091	p	0.0007	713	0.0178	5	60123.2646	s	0.0003	1404.5	0.0400	5
59386.9421	s	0.0007	713.5	0.0180	5						

References: (1) Paschke (2009); (2) O - C gateway; (3) GCVS; (4) Paschke (2010); (5) This work.

The O - C diagram of NW Aps is displayed in the upper panel of Fig. 2, and the solid circles refer to the $O - C$ values calculated from Equation 1. The times of minima cover over the past 30 years. It is obviously to see that linear correction and parabola model can not explain the O - C variations well. Thus, a cyclic variation is also considered. The O - C variation can be expressed as follows:

$$O - C = \Delta T + \Delta P \times E + \frac{1}{2} \times \frac{dP}{dt} \times E^2 + \tau, \quad (2)$$

where ΔT and ΔP are corrections to the initial epoch and initial orbital period used in Equation 1, and $\frac{dP}{dt}$ refers to the parabola changes in the O - C curve. τ represents the periodic variations resulting from light-travel time effect (Irwin 1952) or the Applegate's mechanism (Applegate 1992), and detailed discussions can be found in Section 6.2. In our case, a circular orbit is reasonable to fit the O - C curve well. Therefore, eccentricity is assumed to be $e = 0$. The periodic variation τ in Irwin (1952) can be simplified as follows:

$$\tau = K \sin(\nu + \omega) \quad (3)$$

and

$$K = \frac{1}{2} [(O - C)_{max} - (O - C)_{min}] = \frac{a \cdot \sin i}{c}, \quad (4)$$

in which K is the semi-amplitude of periodic variation and c is the speed of light. Finally, the new ephemeris is determined to be:

$$\begin{aligned} Min.I &= 2458626.6569(\pm 0.0001) + 1.06557319(\pm 0.00000006) \times E \\ &+ 1.630(\pm 0.008) \times 10^{-9} \times E^2 \\ &+ 0.0136(\pm 0.0001) \times \sin[0.0458(\pm 0.0002) \times E - 37.8(\pm 0.6)^\circ] \end{aligned} \quad (5)$$

According to the newly determined ephemeris, the period of NW Aps is revealed to be increasing continuously at a rate of $dP/dt = +1.117(\pm 0.005) \times 10^{-6} day \cdot year^{-1}$. In the upper panel of Fig. 2, the solid line represents the theoretical O - C curve expressed by Equation 5, and the dashed line denotes to the long-term increase in the orbital period. In the middle panel of Fig. 2, the periodic variation is clearly to be seen after the trend of long-term increase is subtracted. The period of cyclic variation is calculated to be $P_3 = 22.9(\pm 0.1)$ and the semi-amplitude is $K = 0.0136(\pm 0.0001)$ day.

4 MODELING OF LIGHT CURVES

The light curves displayed in Fig. 1 cover many orbital period circles. For each sector, we folded the observational data into one orbital circle. The PDCSAP flux is normalized and converted to magnitude as shown in Fig. 3, and the solid circles represent TESS observational light curves. The Wilson-Devinney (WD) code is used to model the light curves (Wilson et al. 2020). Mode 3 for contact configuration is applied since the light curves are typical EW-type. The mass ratio can be achieved with very high reliability since the light curves show totally eclipsing character (Terrell & Wilson 2005). The effective temperature of the star eclipsed at the primary minimum is fixed at $T_1 = 5792K$, which was given in Gaia DR3 (Gaia Collaboration et al. 2023). The gravity-darkening coefficients are set at $g_1 = g_2 = 0.32$ (Lucy 1967). The bolometric albedo coefficients are set at $A_1 = A_2 = 0.5$ (Ruciński 1969). The limb darkening coefficients are set accordingly (van Hamme 1993). The adjustable parameters are mass ratio (q), orbital inclination (i), modified dimensionless surface potential of the primary star (Ω_1), mean surface temperature of the secondary star (T_2), bandpass luminosity of the primary star (L_1). The third light (l_3) is also set to be a free parameter while running the code. However, the fitting results did not improve significantly. Considering that the parameter values of CROWDSAP in TESS Target Pixel Files' headers are over 97% for NW Aps, the model without third light is adopted. The determined photometric parameters are listed in Table 2. Ω_2 refers to the modified dimensionless surface potential of the secondary star, and $\Omega_1 = \Omega_2$ for contact model. Ω_{in} and Ω_{out} are the potential at the inner Lagrangian point and outer Lagrangian point, respectively. ΔT is the temperature difference between the primary and secondary star. L_2 represent the luminosity of the secondary star. $r_1(pole)$, $r_1(side)$ and $r_1(back)$ are three characteristic radii of the primary star in Roche geometry, since stars in close binaries are non-spherical shape. $r_2(pole)$, $r_2(side)$ and $r_2(back)$ are three characteristic radii of the secondary star. And all radii listed in Table 2 are scaled to the semimajor axis (a). The fill-out factor (f) is calculated with the equation $f = \frac{\Omega_{in} - \Omega_1}{\Omega_{in} - \Omega_{out}}$. The fitting residuals are listed in the last line. The theoretical light curves are displayed in Fig. 3 in red line.

5 SYNTHESIS OF SPECTRAL ENERGY DISTRIBUTION

Spectral Energy Distribution (SED) shows the energy emitted by stars as a function of wavelength across the electromagnetic spectrum. It's a powerful tool to study the physical properties of stars. To fitting the SED of NW Aps, photometric observations from a variety of sky survey catalogs are combined, including SkyMapper (Wolf et al. 2018), Gaia Early Data Release 3 (Gaia Collaboration et al. 2021), Gaia Data Release 2 (Gaia Collaboration et al. 2018), AAVSO Photometric All-Sky Survey (Henden et al. 2009), Strömgren-Crawford uvby β photometry (Pauzen 2015), Wide-field Infrared Survey Explorer (Wright et al.

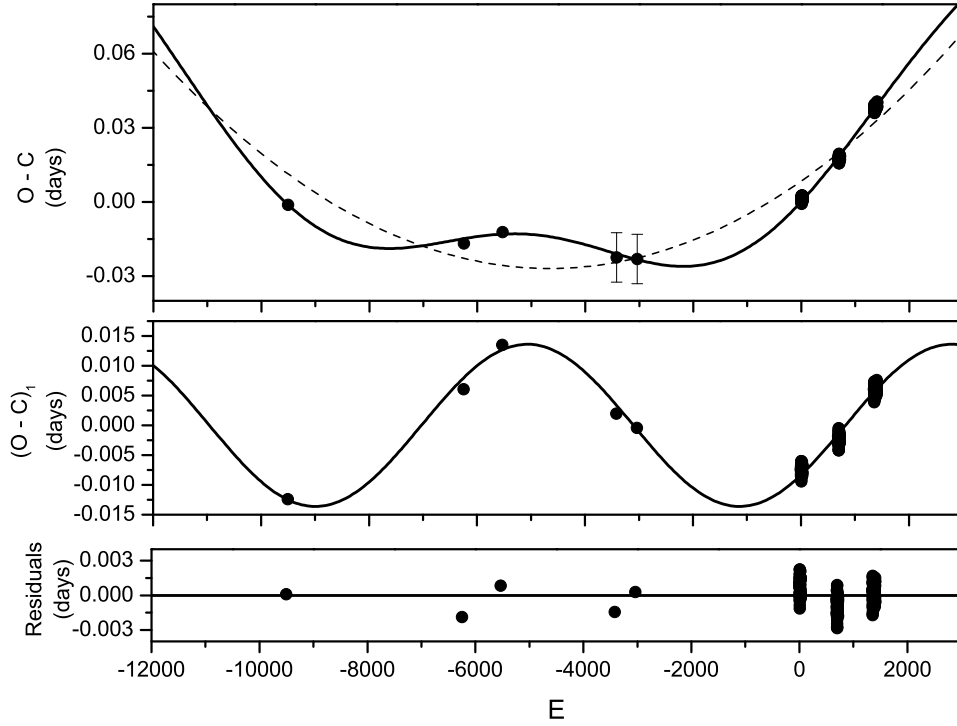


Figure 2. The O - C diagram of NW Aps. In the upper panel, the solid line represents the theoretical O - C curve expressed by Equation 5, and the dashed line denotes the quadratic part. In the middle panel, the periodic variation is clearly to be seen after the trend of quadratic variation is subtracted. The residuals are shown in the bottom after both quadratic and periodic variations are removed.

Table 2. Photometric solutions for NW Aps

Parameters	Sector 12	Sector 39	Sector 65	Sector 66	Averaged
T_1 (K)	5792(fixed)	5792(fixed)	5792(fixed)	5792(fixed)	5792(fixed)
q (M_2/M_1)	0.086(± 0.001)	0.086(± 0.001)	0.085(± 0.001)	0.087(± 0.001)	0.086(± 0.001)
i ($^\circ$)	80.6(± 0.2)	80.8(± 0.6)	80.8(± 0.2)	80.9(± 0.3)	80.8(± 0.3)
Ω_{in}	1.915	1.915	1.910	1.917	1.914
Ω_{out}	1.858	1.859	1.855	1.860	1.856
$\Omega_1 = \Omega_2$	1.870(± 0.001)	1.872(± 0.005)	1.865(± 0.001)	1.874(± 0.002)	1.870(± 0.002)
T_2 (K)	5514(± 6)	5555(± 13)	5512(± 4)	5522(± 6)	5526(± 7)
ΔT (K)	278	237	280	270	266
T_2/T_1	0.952(± 0.001)	0.959(± 0.002)	0.952(± 0.001)	0.953(± 0.001)	0.954(± 0.001)
$L_1/(L_1 + L_2)$	0.9051(± 0.0001)	0.9031(± 0.0001)	0.9056(± 0.0001)	0.9043(± 0.0001)	0.9045(± 0.0001)
l_3	0	0	0	0	0
r_1 (pole)	0.5572(± 0.0005)	0.5563(± 0.0012)	0.5583(± 0.0001)	0.5564(± 0.0006)	0.5571(± 0.0006)
r_1 (side)	0.6332(± 0.0009)	0.6316(± 0.0021)	0.6349(± 0.0002)	0.6318(± 0.0010)	0.6329(± 0.0011)
r_1 (back)	0.6538(± 0.0009)	0.6521(± 0.0021)	0.6556(± 0.0002)	0.6524(± 0.0010)	0.6535(± 0.0011)
r_2 (pole)	0.1983(± 0.0035)	0.1985(± 0.0074)	0.1985(± 0.0002)	0.1980(± 0.0037)	0.1983(± 0.0037)
r_2 (side)	0.2087(± 0.0044)	0.2090(± 0.0092)	0.2092(± 0.0002)	0.2084(± 0.0046)	0.2088(± 0.0046)
r_2 (back)	0.2724(± 0.0189)	0.2726(± 0.0397)	0.2772(± 0.0009)	0.2696(± 0.0186)	0.2730(± 0.0195)
f	78.3 % (± 4.0 %)	77.0 % (± 8.8 %)	82.4 % (± 0.7 %)	75.9 % (± 4.3 %)	78.4 % (± 4.5 %)
$\Sigma \omega(O - C)^2$	0.001183	0.001087	0.001288	0.001229	0.001197

2010) and Two Micron All Sky Survey (Skrutskie et al. 2006). Then, the Python package Speedyfit¹ is applied to fit the observations (Vos et al. 2012). As shown in Table 2, the mass ratio of NW Aps is quite small and the secondary star contribute less than 10% of the total luminosity. NW Aps shows a contact configuration, and both of the two component are embedded in their common envelope. Therefore, it is reasonable to assume that all the electromagnetic radiation come from the primary star and take the binary system as a single star during the fitting. The parallax, effective temperature and surface gravity are adopted from Gaia Data Release 3 (Gaia Collaboration et al. 2023), which are $p = 3.7507 \pm 0.0116 mas$, $T_{eff} = 5792_{-20}^{+23} K$ and $logg = 3.4858_{+0.0037}^{-0.0034}$. Then,

¹ <https://speedyfit.readthedocs.io/en/latest/>

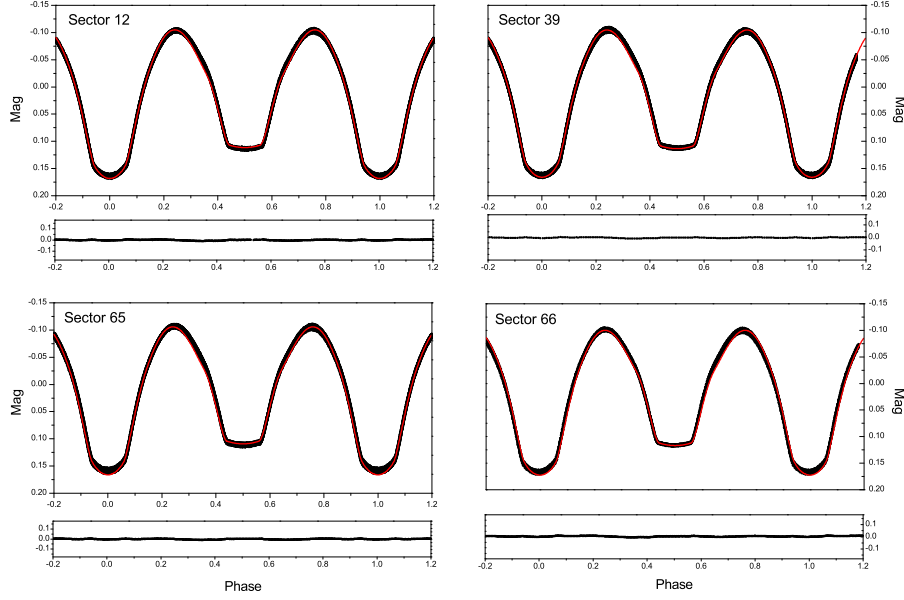


Figure 3. The observational (black dots) and synthetic (red lines) light curves of NW Aps. The residuals are displayed under the light curves.

the zero-point correction to the Gaia DR3 parallax is calculated to be $\Delta p = -0.0123\text{mas}$ with the python package *gaiadr3_zeropoint*², which used the method described in [Lindgren \(2020\)](#) & [Lindgren et al. \(2021\)](#). Thus, the parallax applied in the SED fitting is updated to be $p' = 3.7630 \pm 0.0116\text{mas}$. The Markov chain Monte Carlo (MCMC) approach is used to fit the requested parameters and their errors. The optimal solution is displayed in Figure 4. The parameter distributions from MCMC approach is shown in Figure 5. The mass of primary star is determined to be $M_1 = 1.32 \pm 0.02 M_\odot$.

6 DISCUSSIONS

6.1 Fundamental properties of NW Aps

NW Aps is a quite bright contact binary in the southern celestial hemisphere and TESS obtained its lightcurves with very high precision. Considering its totally eclipsing character, we can conclude that the parameters determined in Table 2 are very reliable ([Li et al. 2021a](#)). NW Aps is a low mass ratio ($q = 0.086$) contact binary system which has approached the minimum mass ratio of contact binary systems. The more fascinating fact is that it may be a stellar merger candidate with the longest orbital period to be reported so far. The mass of the more massive component in NW Aps is determined to be $M_1 = 1.32(\pm 0.02) M_\odot$ from SED fitting. The other absolute parameters of two component stars are calculated and listed in Table 3. The orbital semi-major axis is calculated to be $a = 4.95(\pm 0.03) R_\odot$.

The orbital period of NW Aps is increasing continuously at a rate of $dP/dt = +1.117(\pm 0.005) \times 10^{-6} \text{day} \cdot \text{year}^{-1}$. Considering the fact that mass transfer between the two component stars generally occurs through inner Lagrangian point (L_2) in contact and semi-contact binary systems, the long term period increasing is supposed to be caused by mass transfer from the less massive component to the more massive one. Assuming a conservative mass transfer case, the mass transfer rate is determined to be $\frac{dM_2}{dt} = -3.36(\pm 0.02) \times 10^{-8} M_\odot/\text{year}$ from the less massive secondary star to the more massive one according to Equation 6. Rapid orbital period changes are expected before stellar merger events, such as in the case of V1309 Sco ([Tylenda et al. 2011](#)) and KIC 9832227 ([Molnar et al. 2017](#)), although the 2022 red nova merger prediction of KIC 9832227 was negated later ([Socia et al. 2018](#)). Comparing the orbital period changes' rate of NW Aps with other W UMa-type contact binaries reported before ([Latković et al. 2021](#)), we can conclude that their period changes' rate are in the same time scale and not as rapid as expected. It seems that these low mass ratio contact binary systems are in a quite stable dynamical state.

$$\frac{dM_2}{dt} = \frac{M_1 M_2}{3p(M_2 - M_1)} \times dp/dt \quad (6)$$

6.2 Cyclic variation in the orbital period

The O - C curve in Figure 2 also reveals that a periodic variation of $P_3 = 22.9(\pm 0.1)$ years is superposed on the quadratic changes. It may be resulted from the light-travel time effect (LTTE) of an additional stellar object orbiting around NW Aps. The third body is in a circular orbit, and the projected orbital radius

² <https://pypi.org/project/gaiadr3-zeropoint/>

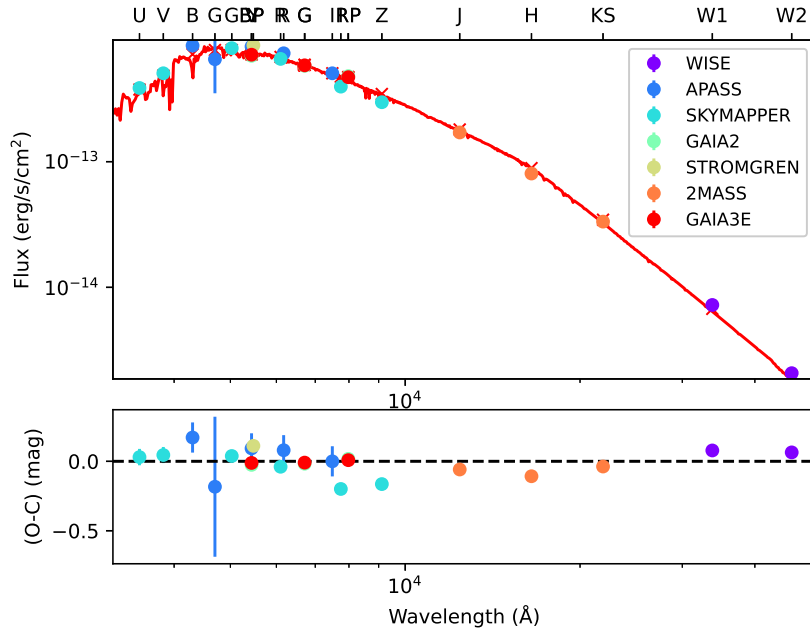


Figure 4. SED fitting of NW Aps. The solid circles represent photometric observations and red line refers to theoretical spectral energy distributions (upper panel). The residuals are displayed in the lower panel.

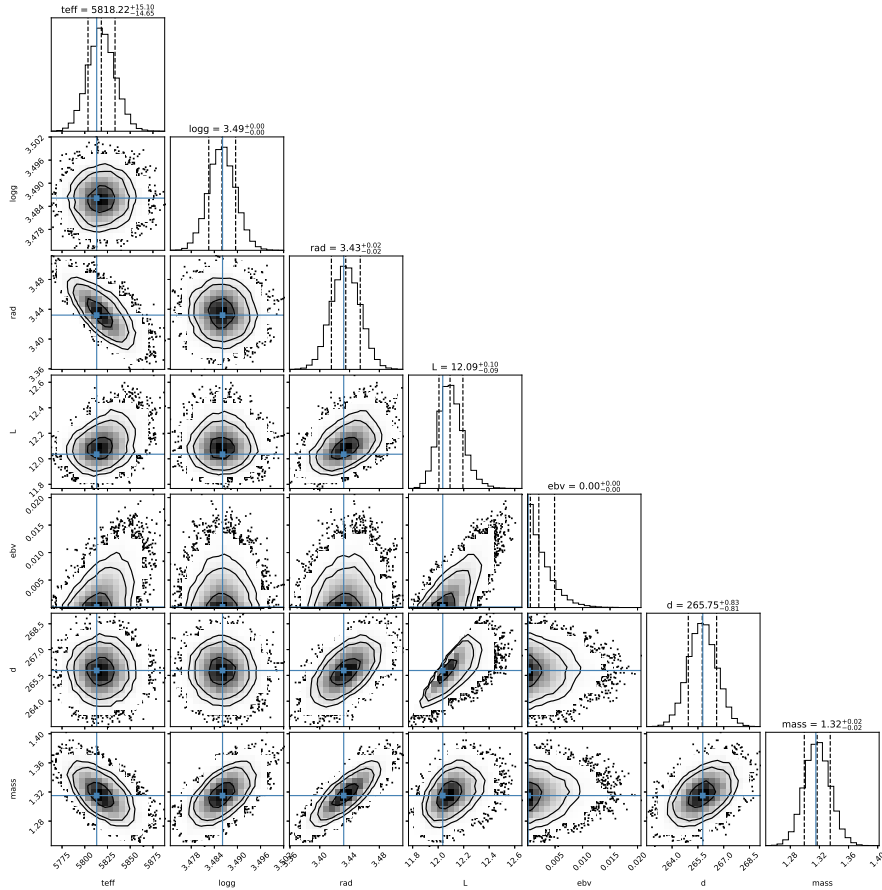
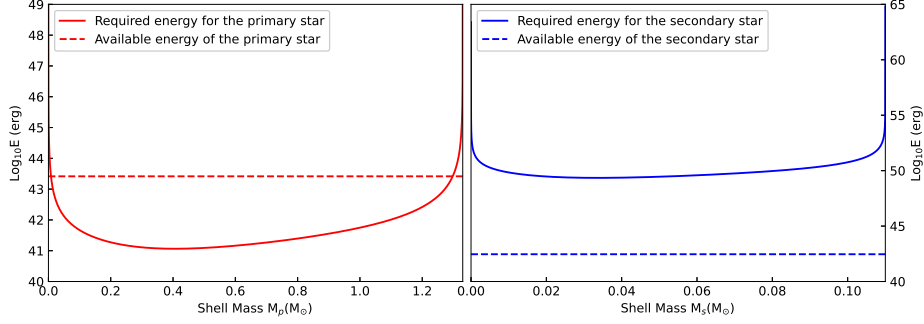


Figure 5. Parameter distributions of the primary star in NW Aps derived from SED fitting.

Table 3. Absolute parameters of components in NW Aps

Parameters	Primary	Secondary
M	$1.32(\pm 0.02)M_{\odot}$	$0.11 \pm 0.01)M_{\odot}$
R	$3.04(\pm 0.02)R_{\odot}$	$1.11(\pm 0.01)R_{\odot}$
L	$9.35(\pm 0.18)L_{\odot}$	$1.04(\pm 0.03)L_{\odot}$


Figure 6. The solid lines correspond to the energy required to generate the detected periodic variation applying the Applegate’s mechanism. The dashed lines represent the radiant energy in a full magnetic activity cycle. Red and blue refer to primary star and secondary one in NW Aps, respectively.

that the central binary NW Aps orbit the barycenter of the triple system is calculated to be $a_{12} \cdot \sin i' = K \times c$, in which K is the semi-amplitude of periodic variation in Equation 5, i' is the orbital inclination of the potential third object, and c is the speed of light. Thus, the projected orbital radius is calculated to be $a_{12} \cdot \sin i' = 2.355(\pm 0.017)AU$. Basing on the Kepler’s third law, the mass function of the potential third object is

$$f(m) = \frac{4\pi^2}{GP_3^2} \cdot (a_{12} \cdot \sin i')^3 = \frac{(M_3 \cdot \sin i')^3}{(M_1 + M_2 + M_3)^2}. \quad (7)$$

G is the gravitational constant, and the value is obtained to be $f(m) = 0.0249(\pm 0.0006)$. Then, the lowest mass of the potential third object is calculated to be $M_3 = 0.436(\pm 0.007)M_{\odot}$, and the orbital radius of the third body is less than $7.73(\pm 0.11)AU$. Since there is no third light detected in the light curves, the potential third object should be a compact object, a white dwarf or a neutron star.

Both of the two component stars in NW Aps are solar-type stars, thus the Applegate’s mechanism resulting from magnetic activity cycle may also cause cyclic variations in the orbital period (Applegate 1992). The Applegate’s mechanism is a theoretical model that explains cyclic orbital period variations observed in close binary systems. Variations in the star’s internal differential rotation and magnetic fields cause changes of its quadrupole moment, which leads to observable oscillations in the orbital period. The approach from Brinkworth et al. (2006) and Völschow et al. (2016) are used to estimated the required energy for the cyclic change. As shown in Figure 6, the energy required to generate the detected periodic variation applying the Applegate’s mechanism are figure out in solid lines and the radiant energy in a full magnetic activity cycle are plotted with dashed lines. It is obviously to state that the cyclic variation may also be cause by the magnetic activity of the primary star.

6.3 Statistics research of extremely low mass ratio contact binaries

Theoretical research predicts that low mass ratio contact binaries stay in the final evolutionary stage of short period contact binaries. They will merge into a rapidly rotating single star and form a FK Com-type star or a blue straggler in the center at last. All well studied totally eclipsing contact binaries with mass ratio $q < 0.1$ are collected and listed in Table 4. They are stellar merger candidates and declared to be merging in the future except the case of V1309 Sco which has merged in 2008. It is easily to be seen that NW Aps has the longest orbital period among the stellar merger candidates and the orbital period of other candidates are shorter than 0.5 days. Although only one target is confirmed to date, the formation and evolution of long period low mass ratio contact binary is really intriguing to us. The surface gravity is calculated with the formula $g = \frac{GM}{R^2}$. The M - R and P - log g relationships of targets listed in Table 4 (except V1309 Sco) are displayed in Fig. 7. In the left panel, the solid line represents the Zero Age Main Sequence (ZAMS) line, while the dashed one refers to the Terminal Age Main Sequence (TAMS) line. The primary stars are still main sequence stars and the secondary stars is oversized to main sequence stars for low mass ratio contact binary with orbital period less than 0.5 days. The secondary stars may have evolved away from main sequence. As for NW Aps, both of the primary and secondary star are oversized to main sequence stars. In the right panel, the surface gravity of the primary and secondary stars in NW Aps are significant lower than main sequence stars. Both of the two component stars may have evolve into red giant stars. And it is obviously to see that there is a gap between short period low mass ratio contact binaries and NW Aps. The P - log g relation is fitted with parabola, which are displayed with blue and green lines for primary stars and secondary stars respectively. The fitting results are :

$$\log g = 0.68(\pm 0.09) \times P^2 - 1.87(\pm 0.12) \times P + 4.81(\pm 0.03) \quad (8)$$

for primary stars, and

$$\log g = 0.78(\pm 0.25) \times P^2 - 2.06(\pm 0.34) \times P + 4.70(\pm 0.09) \quad (9)$$

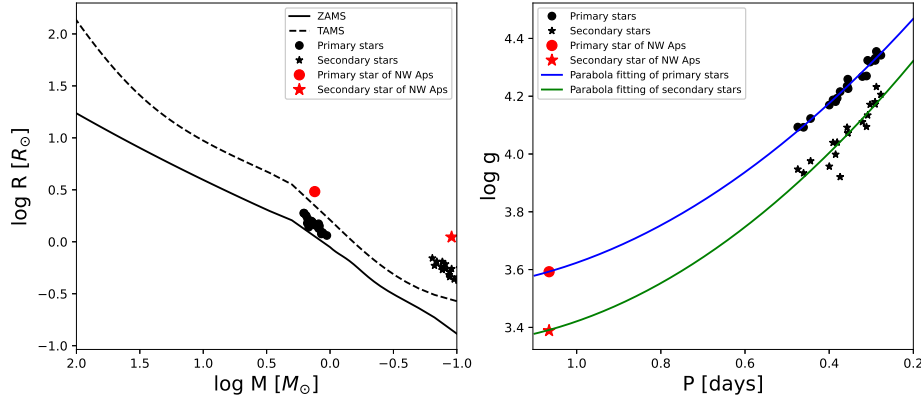
for secondary stars.

The ratio of the spin angular momentum to the orbital angular momentum can be calculated with Equation 10 from Pribulla (1998), in which $r_{1,2}$ and $k_{1,2}$ are the relative radii and dimensionless gyration radii for both component stars respectively. The values are calculated to be $\frac{J_{spin}}{J_{orb}} = 0.307$ or $\frac{J_{orb}}{J_{spin}} = 3.257$ while k_1^2

Table 4. Totally eclipsing contact binaries with mass ratio $q < 0.1$.

Star	Period (days)	q	T_1 K	T_2 K	f %	M_1 M_\odot	M_2 M_\odot	R_1 R_\odot	R_2 R_\odot	L_1 L_\odot	L_2 L_\odot	A R_\odot	dP/dt day \cdot year $^{-1}$	Ref.
V1309 Sco	1.445600	0.094	4500	4354	89									1
NW Aps	1.065558	0.086	5792	5526	60	1.32	0.11	3.04	1.11	9.35	1.04	4.95	$+1.117 \times 10^{-6}$	2
CRTS J162327.1+031900	0.4745615	0.097	6914	6380	27	1.612	0.156	1.888	0.695	6.337	0.873	3.097		3
CRTS J155009.2+493639	0.4609100	0.082	6619	6199	19	1.599	0.130	1.882	0.644	6.429	0.773	3.015	$+6.22 \times 10^{-7}$	3
CRTS J223837.9+321932	0.4441697	0.093	6919	6756	45	1.541	0.144	1.784	0.646	5.463	0.704	2.916	$+5.27 \times 10^{-7}$	3
V870 Ara	0.399722	0.082	5860	6210	96	1.503	0.123	1.67	0.61	2.96	0.50	2.686		4
CRTS J164000.2+491335	0.3907817	0.095	7137	6574	29	1.402	0.133	1.580	0.577	3.912	0.512	2.596	-3.19×10^{-7}	3
1SWASP J132829.37+555246.1	0.384705	0.089	6300	6319	70	1.23	0.11	1.49	0.55	3.15	0.43	2.45	-4.46×10^{-7}	5
V857 Her	0.382230	0.065	8300	8513	84								$+2.90 \times 10^{-7}$	6
CRTS J155106.5+303534	0.3809891	0.089	7147	6819	69	1.384	0.122	1.559	0.552	3.806	0.468	2.537	-5.13×10^{-7}	7
ZZ PsA	0.37388	0.078	6514	6703	97	1.213	0.095	1.422	0.559	2.20	0.63	2.387		3
CRTS J160755.2+332342	0.3572878	0.099	7987	7476	36	1.310	0.130	1.445	0.537	3.053	0.414	2.394		3
ASASSN-V J071924.64+415705.4	0.355763	0.099	5894	6363	88	1.51	0.15	1.51	0.59	2.47	0.41	3.097	-6.70×10^{-7}	8
CRTS J154254.0+324652	0.3549879	0.087	5885	6067	94	1.317	0.114	1.464	0.514	3.215	0.389	2.379	-8.44×10^{-7}	3
CRTS J224827.6+341351	0.3210262	0.079	6077	5541	92	1.233	0.098	1.350	0.456	2.613	0.292	2.171	$+7.71 \times 10^{-6}$	3
ASAS J083241+2332.4	0.311321	0.065	6300	6667	51	1.22	0.08	1.34	0.42	2.66	0.25	2.111	$+8.80 \times 10^{-7}$	9
V1187 Her	0.310766	0.044	6250	6651	80								-1.50×10^{-7}	10
V53 in NGC 6121	0.308449	0.078	7415	6611	69	1.472	0.115	1.383	0.481	7.306	0.465	2.24	-5.89×10^{-7}	11
CRTS J133031.1+161202	0.3026661	0.098	5860	6019	56	1.162	0.114	1.237	0.459	2.018	0.271	2.059		3
CRTS J170307.9+020101	0.2908836	0.093	5433	5237	70	1.134	0.105	1.204	0.436	1.874	0.271	1.985	$+2.54 \times 10^{-7}$	3
CRTS J234634.7+222824	0.2906934	0.086	5851	5746	37	1.141	0.098	1.218	0.425	1.953	0.233	1.964	$+2.19 \times 10^{-7}$	3
NSVS 2569022	0.287797	0.078	6100	6100	1	1.17	0.09	1.19	0.38	1.73	0.17	1.98		12
VSX J082700.8+462850	0.277158	0.055	5870	5728	19	1.06	0.06	1.15	0.32	1.40	0.11	1.83	-9.52×10^{-7}	5

References: (1) [Zhu et al. \(2016\)](#); (2) the present work; (3) [Liu et al. \(2023\)](#); (4) [Szalai et al. \(2007\)](#); (5) [Li et al. \(2021b\)](#); (6) [Qian et al. \(2005\)](#); (7) [Wadhwa et al. \(2021\)](#); (8) [Li et al. \(2022\)](#); (9) [Sriram et al. \(2016\)](#); (10) [Caton et al. \(2019\)](#); (11) [Li et al. \(2017\)](#); (12) [Kjurkchieva et al. \(2018\)](#).

**Figure 7.** The $M - R$ and $P - \log g$ diagrams for totally eclipsing contact binaries with mass ratio $q < 0.1$.

$= k_2^2 = 0.06$ are assumed ([Li & Zhang 2006](#)). Thus, NW Aps is still in a stable state since its orbital angular momentum (J_{orb}) is larger than 3 times of the total spin angular momentum (J_{spin}). NW Aps may become unstable and merge as in the case of V1309 Sco at last, which are predicted by the evolutionary theory of low mass ratio contact binaries. However, considering the particularity in NW Aps, its real evolutionary scenario is still uncertain to us. More photometric and spectroscopic observations will be carried out to reveal some more details on this target in the future. And also, more long period low mass ratio contact binaries, particularly targets in the gap, are needed to be confirmed from sky survey data, which may have great significance in understanding the formation and evolution of long period low mass ratio contact binary.

$$\frac{J_{spin}}{J_{orb}} = \frac{1+q}{q} \times [(k_1 r_1)^2 + q(k_2 r_2)^2] \quad (10)$$

7 CONCLUSIONS

Basing on the solutions derived from TESS light curve and SED fitting, we conclude that NW Aps is an extremely low mass ratio solar-type contact binary. It may lie in the final evolutionary stage of low mass binary systems, and may merger into a rapidly rotating star accompany with luminous optical outburst as theoretical predicted ([Hut 1980](#)). Stellar mergers are extremely energetic events in the Universe, normally accompanying with strong outburst and leading to the formation of peculiar stars, or sometimes triggering a supernova or other explosive phenomena ([Langer 2012](#); [Han et al. 2020](#); [Marchant & Bodensteiner 2024](#)). Merger of compact binaries have gained plenty of attentions since they are typical potential gravitational wave candidates ([Abbott et al. 2016, 2017](#)). However, our knowledge in relation to merger of low mass binary system is still far from adequate. It's very hard to catch the merger events of low mass binary

like V1309 Sco. Thus, efforts are trying to searching their potential progenitor, namely extremely low mass ratio contact binary systems (Yang & Qian 2015; Christopoulou et al. 2022). In the present work, we can see that almost all reported extremely low mass ratio contact binary are in a quite short orbital period less than 0.5 day. NW Aps is the only stellar merger candidate with orbital period longer than 1 day, and it indeed demonstrate some peculiarities, making it worth to study further. In the next step, we will make more efforts in capturing stellar merger candidates or even stellar merge events to enrich our understanding in low mass star evolutions.

ACKNOWLEDGEMENTS

I sincerely appreciate the reviewer's thoughtful and valuable suggestions, which have significantly enhanced the quality of this work. This work is supported by the International Partnership Program of Chinese Academy of Sciences (No. 020GJHZ2023030GC), the Young Talent Project of Yunnan Revitalization Talent Support Program, and the Yunnan Fundamental Research Projects (Grant Nos. 202401AW070004, 202503AP140013, 202401AS070046). This research has made use of the SIMBAD database, operated at CDS, Strasbourg, France. This paper has made use of data collected by the Transiting Exoplanet Survey Satellite (TESS) mission, for which funding is provided by the NASA Explorer Program. All the TESS data used in this paper can be found in MAST: 10.17909/t9-nmc8-f686.

DATA AVAILABILITY

The TESS data are available at <https://archive.stsci.edu/missions-and-data/tess>. All data used in the present paper will be shared on reasonable request to the corresponding author.

REFERENCES

- Abbott B. P., et al., 2016, *Phys. Rev. Lett.*, **116**, 241102
- Abbott B. P., et al., 2017, *ApJ*, **848**, L13
- Applegate J. H., 1992, *ApJ*, **385**, 621
- Arbutina B., 2007, *Monthly Notices of the Royal Astronomical Society.*, **377**, 1635
- Bellm E. C., et al., 2019, *Publications of the Astronomical Society of the Pacific*, **131**, 018002
- Brinkworth C. S., Marsh T. R., Dhillon V. S., Knigge C., 2006, *MNRAS*, **365**, 287
- Brown N. J., Waagen E. O., Scovill C., Nelson P., Oksanen A., Solonen J., Price A., 2002, *IAU Circ.*, **7785**, 1
- Caldwell D. A., et al., 2020, *Research Notes of the American Astronomical Society*, **4**, 201
- Caton D., Gentry D. R., Samec R. G., Chamberlain H., Robb R., Faulkner D. R., Hill R., 2019, *Publications of the Astronomical Society of the Pacific*, **131**, 054203
- Chen X., Han Z., 2008, *Monthly Notices of the Royal Astronomical Society.*, **387**, 1416
- Chen X., Wang S., Deng L., de Grijs R., Yang M., 2018, *ApJS*, **237**, 28
- Chen X., Wang S., Deng L., de Grijs R., Yang M., Tian H., 2020, *ApJS*, **249**, 18
- Christopoulou P.-E., Lalounta E., Papageorgiou A., Ferreira Lopes C. E., Catelan M., Drake A. J., 2022, *Monthly Notices of the Royal Astronomical Society.*, **512**, 1244
- Ferreira T., Saito R. K., Minniti D., Navarro M. G., Ramos R. C., Smith L., Lucas P. W., 2019, *Monthly Notices of the Royal Astronomical Society.*, **486**, 1220
- Gaia Collaboration et al., 2018, *A&A*, **616**, A1
- Gaia Collaboration et al., 2021, *A&A*, **649**, A1
- Gaia Collaboration et al., 2023, *Astronomy and Astrophysics*, **674**, A1
- Gazeas K. D., et al., 2021, *Monthly Notices of the Royal Astronomical Society.*, **502**, 2879
- Han Z.-W., Ge H.-W., Chen X.-F., Chen H.-L., 2020, *Research in Astronomy and Astrophysics*, **20**, 161
- Hayashi S. S., Yamamoto M., Hirose K., 1994, *IAU Circ.*, **5942**, 1
- Henden A. A., Welch D. L., Terrell D., Levine S. E., 2009, in *American Astronomical Society Meeting Abstracts #214*. p. 407.02
- Huang S.-S., 1963, *ApJ*, **138**, 471
- Hut P., 1980, *Astronomy and Astrophysics*, **92**, 167
- Irwin J. B., 1952, *ApJ*, **116**, 211
- Ivanova N., et al., 2013, *Astronomy and Astrophysics*, **21**, 59
- Jenkins J. M., et al., 2016, in Chiozzi G., Guzman J. C., eds, *Society of Photo-Optical Instrumentation Engineers (SPIE) Conference Series Vol. 9913, Software and Cyberinfrastructure for Astronomy IV*. p. 99133E, doi:10.1117/12.2233418
- Kjurkchieva D. P., Popov V. A., Petrov N. I., 2018, *Research in Astronomy and Astrophysics*, **18**, 129
- Kochanek C. S., Adams S. M., Belczynski K., 2014, *Monthly Notices of the Royal Astronomical Society.*, **443**, 1319
- Kwee K. K., van Woerden H., 1956, *Bull. Astron. Inst. Netherlands*, **12**, 327
- Langer N., 2012, *ARA&A*, **50**, 107
- Latković O., Čeki A., Lazarević S., 2021, *The Astrophysical Journals*, **254**, 10
- Li L., Zhang F., 2006, *Monthly Notices of the Royal Astronomical Society.*, **369**, 2001
- Li K., Hu S., Chen X., Guo D., 2017, *Publications of the Astronomical Society of Japan*, **69**, 79
- Li K., et al., 2021a, *The Astronomical Journal*, **162**, 13
- Li K., Xia Q.-Q., Kim C.-H., Hu S.-M., Guo D.-F., Jeong M.-J., Chen X., Gao D.-Y., 2021b, *The Astrophysical Journal*, **922**, 122
- Li K., Gao X., Liu X.-Y., Gao X., Li L.-Z., Chen X., Sun G.-Y., 2022, *The Astronomical Journal*, **164**, 202
- Lightkurve Collaboration et al., 2018, *Lightkurve: Kepler and TESS time series analysis in Python*, *Astrophysics Source Code Library*, record ascl:1812.013 (ascl:1812.013)
- Lindgren L., 2020, *A&A*, **633**, A1
- Lindgren L., et al., 2021, *A&A*, **649**, A4

- Liu X.-Y., et al., 2023, *Monthly Notices of the Royal Astronomical Society*, 519, 5760
- Lucy L. B., 1967, *Zeitschrift fur Astrophysik*, 65, 89
- Marchant P., Bodensteiner J., 2024, *ARA&A*, 62, 21
- Molnar L. A., et al., 2017, *The Astrophysical Journal*, 840, 1
- Nakano S., Nishiyama K., Kabashima F., Sakurai Y., 2008, *Central Bureau Electronic Telegrams*, 1496, 1
- Paschke A., 2009, *Open European Journal on Variable Stars*, 0116, 1
- Paschke A., 2010, *Open European Journal on Variable Stars*, 130, 1
- Paunzen E., 2015, *A&A*, 580, A23
- Pejcha O., Metzger B. D., Tomida K., 2016, *Monthly Notices of the Royal Astronomical Society*, 455, 4351
- Pojmanski G., 1997, *Acta Astronomica*, 47, 467
- Pribulla T., 1998, *Contributions of the Astronomical Observatory Skalnaté Pleso*, 28, 101
- Prša A., et al., 2022, *ApJS*, 258, 16
- Qian S., 2001, *MNRAS*, 328, 635
- Qian S. B., Zhu L. Y., Soonthornthum B., Yuan J. Z., Yang Y. G., He J. J., 2005, *The Astronomical Journal*, 130, 1206
- Qian S. B., Liu L., Zhu L. Y., He J. J., Yang Y. G., Bernasconi L., 2011, *The Astronomical Journal*, 141, 151
- Ricker G. R., et al., 2015, *Journal of Astronomical Telescopes, Instruments, and Systems*, 1, 014003
- Ruciński S. M., 1969, *Acta Astronomica*, 19, 245
- Skrutskie M. F., et al., 2006, *AJ*, 131, 1163
- Socia Q. J., Welsh W. F., Short D. R., Orosz J. A., Angione R. J., Windmiller G., Caldwell D. A., Batalha N. M., 2018, *The Astrophysical Journal*, 864, L32
- Sriram K., Malu S., Choi C. S., Vivekananda Rao P., 2016, *The Astronomical Journal*, 151, 69
- Strohmeier W., Patterson I., 1969, *Information Bulletin on Variable Stars*, 330, 1
- Szalai T., Kiss L. L., Mészáros S., Vinkó J., Csizmadia S., 2007, *Astronomy and Astrophysics*, 465, 943
- Terrell D., Wilson R. E., 2005, *Astrophysics and Space Science*, 296, 221
- Tylenda R., et al., 2011, *Astronomy and Astrophysics*, 528, A114
- Tylenda R., et al., 2013, *Astronomy and Astrophysics*, 555, A16
- Udalski A., Szymanski M., Kaluzny J., Kubiak M., Mateo M., 1992, *Acta Astronomica*, 42, 253
- Völschow M., Schleicher D. R. G., Perdelwitz V., Banerjee R., 2016, *A&A*, 587, A34
- Vos J., et al., 2012, *A&A*, 548, A6
- Wadhwa S. S., 2005, *Astrophysics and Space Science*, 300, 329
- Wadhwa S. S., De Horta A., Filipović M. D., Tothill N. F. H., Arbutina B., Petrović J., Djurašević G., 2021, *Monthly Notices of the Royal Astronomical Society*, 501, 229
- Wilson R. E., Devinney E. J., Van Hamme W., 2020, WD: Wilson-Devinney binary star modeling, *Astrophysics Source Code Library*, record ascl:2004.004 (ascl:2004.004)
- Wolf C., et al., 2018, *Publ. Astron. Soc. Australia*, 35, e010
- Wright E. L., et al., 2010, *AJ*, 140, 1868
- Yang Y.-G., Qian S.-B., 2015, *The Astronomical Journal*, 150, 69
- Zhu L.-Y., Zhao E.-G., Zhou X., 2016, *Research in Astronomy and Astrophysics*, 16, 68
- van Hamme W., 1993, *The Astronomical Journal*, 106, 2096

This paper has been typeset from a $\text{\TeX}/\text{\LaTeX}$ file prepared by the author.